

Determination of the Composition of the Universe Using Type Ia Supernovae

KATIE N. BROWN¹ AND AIDAN A. SIRBU¹

¹*Western University*

1151 Richmond St,

London, ON N6A 3K7, Canada

ABSTRACT

The objective of this investigation is to study the acceleration of the expansion of the universe by determining the relative energy densities of dark energy and matter. Using type Ia supernovae as standard candles, we analyse measurements of their redshift and apparent magnitude in the B-band. We first fit a simple model for $m_B(z)$ in the low redshift limit to the $z \leq 0.1$ data and determine that type Ia supernovae have an effective blue-band absolute magnitude of $\mathcal{M}_B = -3.19 \pm 0.07$. We then construct a general relativistic model for $m_B(z; \Omega_{M,0}, \Omega_{\Lambda,0})$ under the assumption of a flat universe. We fit the data to this model both with and without the constraint that $\Omega_{M,0} + \Omega_{\Lambda,0} = 1$ and find that the unconstrained fits have higher coefficients of determination and are therefore, likely, better quality fits. When fitting this model to the data-set from [Perlmutter et al. \(1999\)](#), the normalized energy densities of matter and dark energy are found to be $\Omega_{M,0} = 0.30$ and $\Omega_{\Lambda,0} = 0.91$. In contrast, when using the updated data-set from [Suzuki et al. \(2012\)](#), which contains many more SNe over a larger range of redshift, these parameters are found to be $\Omega_{M,0} = 0.73$ and $\Omega_{\Lambda,0} = 0.16$. This result supports a mass-based, decelerating universe, contradicting the common idea of accelerating expansion driven by dark energy.

1. INTRODUCTION

Cosmology is the study of the evolution and large-scale properties of the universe ([Tillman & Harvey 2022](#)). One of the biggest ideas in cosmology is the expansion of the universe, first discovered by Edwin Hubble in 1929. He proposed that space itself is expanding, causing all astronomical bodies to recede from one another, countered by gravitational attraction on the local scale. Even the wavelength of light is increased as it travels through the expanding space, producing a cosmological redshift.

Another important piece in the foundation of cosmology is Einstein's Theory of General Relativity, which explains gravitation as the warping of spacetime by massive bodies. General Relativity claims that the geometry of the universe can take three forms: a closed model with positive curvature (like a sphere), an open universe with negative curvature (like a saddle), or a flat universe with no large-scale curvature ([Cottier 2021](#)). This geometry has a significant impact on the form of the equations used in cosmological models, especially those pertaining to the expansion of the universe. Current astronomical evidence, including measurements of the cosmic microwave background (CMB) and baryon acoustic oscillations, support the flat universe model ([Cottier 2021](#)).

Standard candles are groups of astrophysical objects with known absolute magnitudes and thus distances that are straightforward to estimate. One of the most commonly used class of standard candles are type Ia Supernovae (SNe). These are a type of SNe whose spectra do not contain hydrogen emission lines, believed to be produced when a white dwarf accreting mass from a binary companion nears the Chandrasekhar limit and collapses. As all type Ia SNe are produced by stars of approximately the same mass, there is exceptional consistency among their light curves and spectra. This allows for accurate determination of distance, even at very high redshift.

One of the most significant recent advancements in cosmology was achieved simultaneously by the Supernova Cosmology Project at Lawrence Berkeley National Laboratory and the international High-Z Supernova Search Team. These groups used type Ia supernovae as standard candles and compared their distances and redshifts. As predicted by the Hubble Law, they found that further sources (those at higher redshifts) are receding faster. Unexpectedly, however, they also found that the rate of recession is increasing; the expansion of the universe appears to be accelerating. Their best-fit model assumed that the universe is geometrically flat, which is aligned with other cosmological evidence ([Perlmutter 2003](#)). They found a positive value for the cosmologi-

cal constant Λ , which describes the repulsive “vacuum energy” of the universe. They suggested that this is produced by a “dark energy” which can vary over time and is driving the acceleration of the expansion of the universe. Both groups determined that the total energy density of the universe is approximately 70% dark energy and 30% mass (both dark and baryonic matter). The leaders of these two research groups shared the 2011 Nobel Prize in Physics for their discovery.

The objective of this paper is to investigate the acceleration of the expansion of the universe and the distribution of its energy density between dark energy and matter. We follow a similar procedure to the previous research described above, using type Ia SNe as standard candles. We analyze two sets of SNe data, both the original 1999 data published by Perlmutter et al., as well as the updated and more robust 2011 dataset Suzuki et al. (2012)¹. We use measurements of apparent magnitude in the B-band and redshift. We first fit the low redshift ($z \leq 0.1$) data to a simple model to estimate the modified absolute B-band magnitude for type Ia SNe. We then fit the complete data to a more complex general relativistic model to determine values for the normalized energy densities of dark energy and matter, Ω_Λ and Ω_M . As will be further discussed, these parameters alone should indicate whether the expansion of the universe is accelerating or decelerating (Perlmutter et al. 1999). This is performed for both an unconstrained model where Ω_Λ and Ω_M can take on any value, and a constrained - flat universe - model in which Ω_Λ and Ω_M must sum to unity. At each point, statistical analysis is performed to assess and compare the quality of the various fits.

2. METHODS

2.1. Determination of modified absolute magnitude in the B-band

In order to determine the best fit value of $\Omega_{M,0}$ and $\Omega_{\Lambda,0}$, one must first determine the modified absolute magnitude in the B-band, \mathcal{M}_B . As type Ia SNe are considered standard candles, they are expected to have a common \mathcal{M}_B . In order to derive a value, an equation which approximates the apparent magnitude, m_B , under a low redshift limit ($z \leq 0.1$) is used as a fitting model with \mathcal{M}_B as the parameter in question. The model equation is

$$m_B(z) = \mathcal{M}_B + 5 \log_{10}(cz) \quad (1)$$

¹ This data was gathered and submitted to be published in 2011, and finally published in 2012

where c , the speed of light, is taken in km/s . Redshift data of $z < 0.1$ is extracted from Perlmutter et al. (1999) and the updated 2011 data set of Suzuki et al. (2012), henceforth referred to as the 1999 and 2011 data-sets, respectively. The least-squares fitting method is implemented using the trust region reflective algorithm in order to yield the fitted models. Furthermore, Matlab provides a 95% confidence interval for each determined parameter. This interval is divided by 4 to yield 1 standard deviation which is then used as uncertainty. Two \mathcal{M}_B values are determined, one from each data set. A weighted average of the two, using the coefficient of determination of each fit as the weights, is taken to be the determined \mathcal{M}_B .

2.2. Determination of unconstrained normalized energy density of matter and dark energy

Using the determined values of \mathcal{M}_B , one can now use the model equation (once again with c taken in km/s)

$$m_B(z) = \mathcal{M}_B + 5 \log_{10} \left[c(1+z) \int_0^z \frac{dz'}{\sqrt{\Omega_{M,0}(1+z')^3 + \Omega_{\Lambda,0}}} \right] \quad (2)$$

to find the best fitting values of $\Omega_{M,0}$ and $\Omega_{\Lambda,0}$.² Both the 1999 and 2011 data-sets are analyzed using the same method. This section involves the use of unconstrained values of normalized energy density which have not been made to sum to unity. In order to fit the data to the model, the model is first coded as a function in Matlab. The function takes $\Omega_{M,0}$ and $\Omega_{\Lambda,0}$ as parameters with z - the independent variable - as an array. The function evaluates the integral in equation (2) using the built in `integral` method. The integration is performed from 0 to z in a loop such that a theoretical apparent magnitude is determined for each redshift value. The model function is then supplied to Matlab’s least-squares solver `lsqcurvefit` along with the redshift values and experimentally determined apparent magnitudes. An initial guess of $\Omega_{M,0} = \Omega_{\Lambda,0} = 0.5$ is also supplied. Both the trust-region-reflective and Levenberg-Marquardt algorithms are used. Furthermore, a rigorous statistical analysis concerning the goodness of fit is also employed.

2.3. Determination of constrained normalized energy density of matter and dark energy

As explained in appendix A, equation (2) is derived under the assumption of a flat universe. Under this flat universe assumption, it is expected that $\Omega_{M,0} + \Omega_{\Lambda,0} \approx 1$.

² For a full derivation of equation (2), see appendix section A

Therefore, the unconstrained approach in the determination of these parameters taken in sections 2.2 and 3.2 is inherently subjected to systematic error as the base assumption is not adhered to. In order to rectify this, a constrained model is used:

$$m_B(z) = \mathcal{M}_B + 5 \log_{10} \left[c(1+z) \int_0^z \frac{dz'}{\sqrt{(1-\Omega_{\Lambda,0})(1+z')^3 + \Omega_{\Lambda,0}}} \right]. \quad (3)$$

where $\Omega_{M,0} = 1 - \Omega_{\Lambda,0}$. Aside from the difference in the model, the same methodology discussed in section 2.2 is employed.

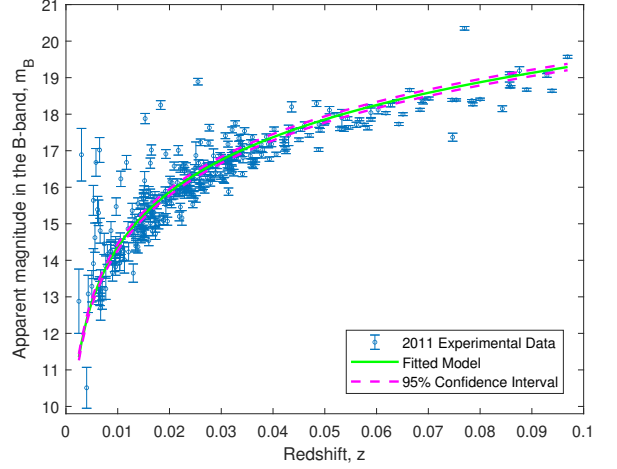
3. RESULTS

3.1. Determination of modified absolute magnitude in the B-band

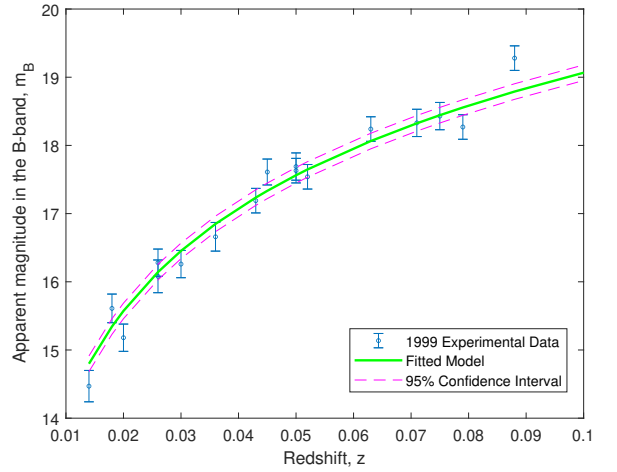
The absolute magnitude in the B-band is determined to be $\mathcal{M}_{B,99} = -3.32 \pm 0.06$ from the 1999 data and $\mathcal{M}_{B,11} = -3.02 \pm 0.04$ for the 2011 data. The data sets, along with their fitted models and confidence intervals are represented in figure 1. Firstly, the uncertainty is smaller for $\mathcal{M}_{B,11}$ than for $\mathcal{M}_{B,99}$. This is as expected since the 2011 data contains many more data points which should increase the certainty of the calculation. However, a quick inspection of figure 1a reveals that the supposed 95% confidence interval barely captures the data as opposed to figure 1b where the confidence interval captures the uncertainty range of every data point save one. Looking at the goodness of fit, it is found that the coefficient of determination, R^2 , of the 2011 data set is $R_{11}^2 = 0.74$ while that of the 1999 data set is $R_{99}^2 = 0.97$. R^2 is a measure of how much of the variance between the model and the experimental data is due to the data itself rather than error in the model (Colin Cameron & Windmeijer 1997). From this, one can conclude that although the 2011 model appears not to capture the majority of its data points, its large R^2 value is evidence that the data itself merely has a large variance. While the 1999 data clearly possesses a better fit, the 2011 fit cannot be disregarded as its coefficient of determination is evidence for a moderate to good fit. A weighted average of each \mathcal{M}_B is therefore taken using the coefficients of determination as the weights. The resulting modified absolute magnitude in the B-band is $\mathcal{M}_B = -3.19 \pm 0.07$, where the uncertainty was propagated using standard practice.

3.2. Determination of unconstrained normalized energy density of matter and dark energy

As previously stated, both the trust region reflective and Levenberg-Marquardt least-squares algorithms are



(a) 2011 Data set (Suzuki et al. 2012)



(b) 1999 Data set (Perlmutter et al. 1999)

Figure 1: Apparent magnitude vs redshift ($z \leq 1$) of various SNe. The model function used to fit the data is $m_B(z) = \mathcal{M}_B + 5 \log cz$. Both the 1999 data set as well as the updated 2011 data set are shown. The determined values of the absolute B-band magnitude are $\mathcal{M}_{B,99} = -3.32 \pm 0.06$ for the 1999 data and $\mathcal{M}_{B,11} = -3.02 \pm 0.04$ for the 2011 data. The 95% confidence interval for the determined \mathcal{M}_B parameter are also represented, but does not appear to capture the data well.

used in order to find the fitted parameters, $\Omega_{M,0}$ and $\Omega_{\Lambda,0}$. Both of the algorithms yield equivalent values for both data sets. Due to this, the statistical analysis is conducted only on the trust region reflective results. For the 2011 data: $\Omega_{M,0,11} = 0.73$ and $\Omega_{\Lambda,0,11} = 0.16$. For the 1999 data: $\Omega_{M,0,99} = 0.30$ and $\Omega_{\Lambda,0,99} = 0.91$. The experimental data for each data-set containing all the redshift values as well as the fitted curves are shown

in figure 2. An odd peculiarity of the data is that the normalized energy density parameters for matter and dark energy, $\Omega_{M,0}$ and $\Omega_{\Lambda,0}$, appear to be almost flipped between the data sets such that $\Omega_{M,0,'11} > \Omega_{\Lambda,0,'11}$ while $\Omega_{M,0,'99} < \Omega_{\Lambda,0,'99}$. While cosmological implications will be discussed, a goodness of fit evaluation must first be employed. The coefficient of determination of the 1999 data and the 2011 data, respectively, are $R^2_{99} = 0.99$ and $R^2_{11} = 0.98$. The 1999 data-set, at first glance, appears to be a more accurate fit. It's coefficient of determination further substantiates that notion, though marginally. However, the small discrepancy in the quality of the fits does not account for the large discrepancies in the normalized energy density parameters predicted by each model.

3.3. Determination of constrained normalized energy density of matter and dark energy

Once again, the Levenberg-Marquardt and trust region reflective least-squares algorithms yield the same normalized energy density parameters. These parameters are found to be $\Omega_{M,0,'11} = 0.58$, $\Omega_{\Lambda,0,'11} = 0.42$ for the 2011 data-set and $\Omega_{M,0,'99} = 0.55$, $\Omega_{\Lambda,0,'99} = 0.45$ for the 1999 data-set. The experimental data for both data-sets and their fitted curves are represented in figure 3. At first glance, the fits in figures 3a and 3b appear almost indistinguishable from those presented in section 3.2. In order to highlight the difference in the fits, a goodness of fit evaluation is performed. The coefficients of the determination for the 1999 and 2011 data-set, respectively, are $R^2_{99} = 0.99$ and $R^2_{11} = 0.97$. Both fits are of equivalent quality as their unconstrained counterpart. The goodness of fit clearly does not provide adequate information to differentiate the constrained and unconstrained models. The remaining two differentiating factors are the model itself (along with its base assumptions) and the resulting normalized energy density parameters. Firstly, as discussed in section 2.3, the base assumption of the constrained model is in line with the assumptions used in order to derive it. By default, it is expected that the constrained model provide a more accurate representation of the parameters. Secondly, the peculiarity in the parameters for the constrained model are not present. Both the 1999 and 2011 data-sets predict that $\Omega_{M,0} > \Omega_{\Lambda,0}$. This consistency further substantiates the notion that the constrained model is superior to the unconstrained.

3.4. Comparison of different normalized energy densities

The experimental data-sets, their respective best fits, as well as various other fits with extreme normalized

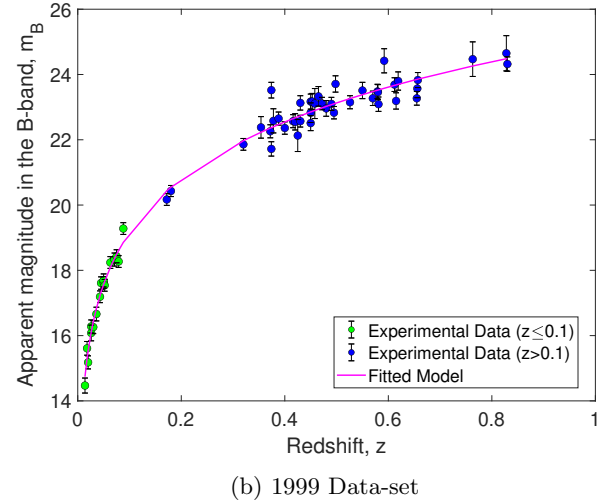
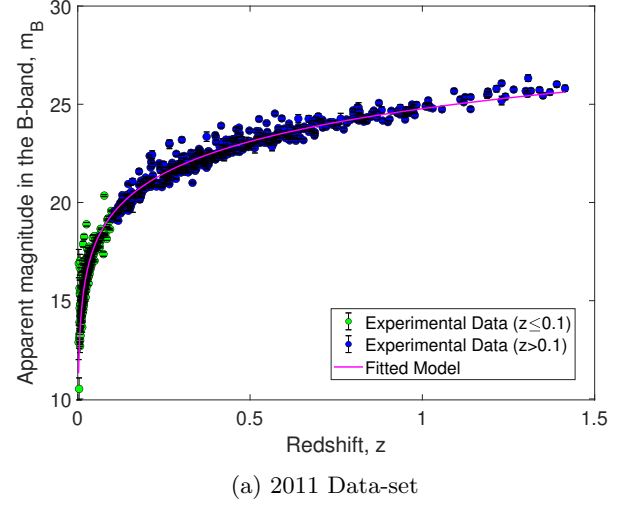
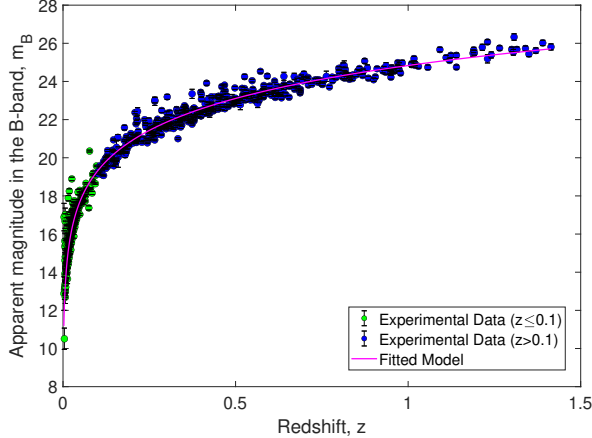
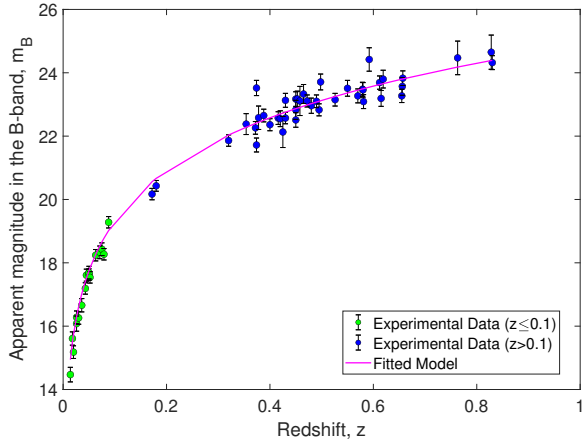


Figure 2: Apparent magnitude vs redshift of various SNe. The green data points represent the low redshift data, while the blue data points represent the high redshift data. The model used to fit the data is equation (2). The determined parameters for 2011 are: $\Omega_{M,0,'11} = 0.73$ and $\Omega_{\Lambda,0,'11} = 0.16$. The determined parameters for 1999 are: $\Omega_{M,0,'99} = 0.30$ and $\Omega_{\Lambda,0,'99} = 0.91$. The 1999 model appears to pass through the majority of the error ranges of each data point. The 2011 model appears to pass through a smaller portion of its data points, however it still appears to fit the overall trend to a high degree.

energy density parameters are represented in figure 4. The best fit for the 2011 model was found to be the unconstrained model by a small margin. Meanwhile, the unconstrained and constrained models for the 1999 data exhibited equivalent goodness of fit. Since the 2011 fit was taken to be unconstrained, the unconstrained fit for



(a) 2011 Data-set



(b) 1999 Data-set

Figure 3: Apparent magnitude vs redshift of various SNe. The green data points represent the low redshift data, while the blue data points represent the high redshift data. The model used the fit the data is equation (3). The determined parameters for 2011 are: $\Omega_{M,0,'11} = 0.58$ and $\Omega_{\Lambda,0,'11} = 0.42$. The determined parameters for 1999 are: $\Omega_{M,0,'99} = 0.55$ and $\Omega_{\Lambda,0,'99} = 0.45$. The fit of the plots appear almost indistinguishable from those in figure 2.

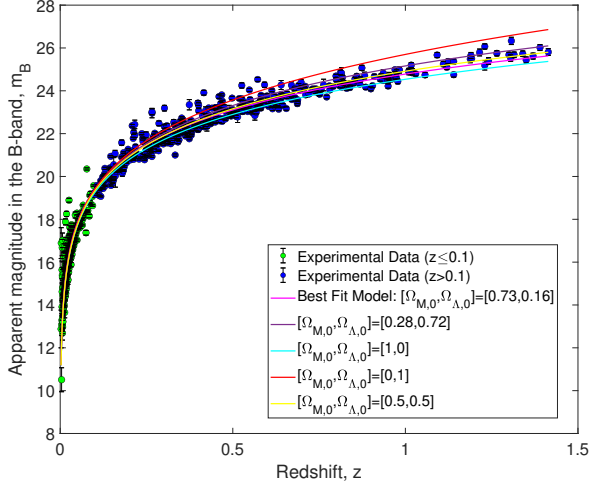
the 1999 data was also chosen. As one can observe, in both figures 4a and 4b, the fit lines begin overlapped, slowly differentiating as redshift increases. The extreme values of $[\Omega_{M,0}, \Omega_{\Lambda,0}] = [0, 1]$ produce the highest trend-line. On the other hand $[\Omega_{M,0}, \Omega_{\Lambda,0}] = [1, 0]$ produce the lowest. From this, one can see that higher values of dark energy density shift the apparent magnitude in the B-band upwards for SNe at high redshifts. Inversely, high values of matter energy density tends to shift apparent magnitudes downwards for higher redshifts. This phe-

nomena is further observed for the best fit models of the 2011 and 1999 data-sets respectively. Using the yellow trend lines with parameters $[\Omega_{M,0}, \Omega_{\Lambda,0}] = [0.5, 0.5]$ as the middle divider, the best fit model for the 2011 data-set predicts higher apparent magnitudes for high redshifts while the best fit model for the 1999 data-set predicts lower. Furthermore, the trend line with normalized energy density parameters determined by Perlmutter et al. (1999) is also shown in both figures 4a and 4b. As expected, since the 1999 data-set was taken from Perlmutter et al. (1999), the best fit line for the 1999 data matches that of Perlmutter et al. (1999) better than the 2011 best fit. Focusing on the 1999 data, the $\Omega_{M,0}$ parameter seems to be in high concordance with that of Perlmutter et al. (1999), but there is a 22% difference between the values of $\Omega_{\Lambda,0}$.

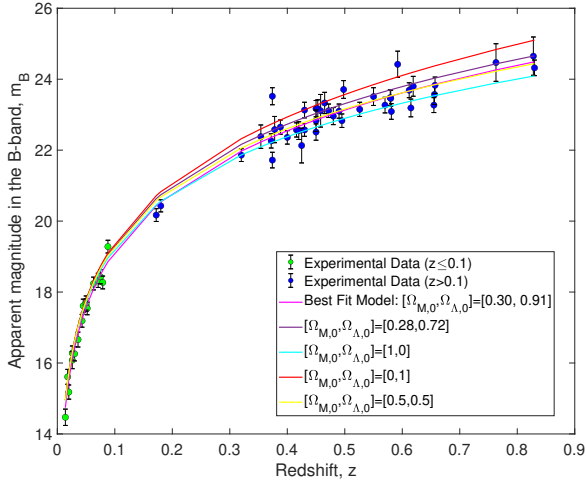
4. DISCUSSION

Perlmutter et al. (1999) discuss many of the systematic uncertainties present in this SNe data. Firstly, while galactic extinction is corrected for, the magnitudes are likely further decreased by extinction by dust in the host galaxy and intergalactic medium. The data is also likely affected by the Malmquist bias, the preferential detection of objects with higher absolute magnitudes. Observed magnitudes could also be distorted by gravitational lensing, due to particularly low or high mass densities along the line-of-sights to the SNe. Additionally, minor changes in spectral features could be caused by evolution of the mass, metallicity and carbon-oxygen ratio of progenitor populations and environments.

Perlmutter et al. (1999) defines the current-deceleration-parameter as $q_0 \equiv \frac{1}{2}\Omega_M - \Omega_\Lambda$. They show that the expansion of the universe is accelerating for $q_0 < 0$ - or, equivalently, $\Omega_\Lambda > \frac{1}{2}\Omega_M$ - and decelerating otherwise. They found $\Omega_M = 0.28$ and $\Omega_\Lambda = 0.72$ for their primary fit, in line with the results of $\Omega_M = 0.32$ and $\Omega_\Lambda = 0.68$ by Riess et al. (1998). Both results strongly support an accelerating expansion. Using the 1999 data, the results from both the unconstrained and constrained models found $\Omega_\Lambda > \frac{1}{2}\Omega_M$, supporting an accelerating universe. This was also consistent with the results from the constrained model fit to the 2011 data. However, fitting the 2011 data to the unconstrained model yields $\Omega_{M,0,'11} = 0.73$ and $\Omega_{\Lambda,0,'11} = 0.16$, which implies a decelerating universe. This inconsistency may be caused by simplifications and self-contradictions in our model. As explained in appendix A, equation (2), which was used as the fitted model, was derived on multiple assumptions of a flat universe. Using that model without enforcing the constraint that the two energy densities sum to unity introduces systematic error as the



(a) 2011 Data-set



(b) 1999 Data-set

Figure 4: Experimental data of 2011 and 1999 data-sets along with their best fit normalized energy density parameters. Also included are a variety of fits which use different extreme values of $\Omega_{M,0}$ and $\Omega_{\Lambda,0}$. Specifically, $[\Omega_{M,0}, \Omega_{\Lambda,0}] = [0.28, 0.72]$, are the best fit parameters deduced by [Perlmutter et al. \(1999\)](#).

assumption is not consistent with its application. Furthermore, differences in the numerical models used likely contributed to inconsistencies with results of previous work. While [Perlmutter et al. \(1999\)](#) do not explicitly state the model being used, the equation being fit in [Riess et al. \(1998\)](#) has key differences from equation 2.

Another key factor that likely contributed to the inconsistencies among our results and compared to other published works was the difference in the two data-sets used. Especially with the unconstrained model, our

analysis of the 2011 data suggested a strongly mass-based universe. This contradicts the analyses of the original 1999 data by [Perlmutter et al. \(1999\)](#) and [Riess et al. \(1998\)](#). While differences in models were likely a contributing factor, it is plausible that differences in the data itself also resulted in the inconsistencies among the results. The 2011 data was far more extensive, containing 714 SNe with redshift values ranging up to 1.414, compared to the 60 SNe ranging up to redshift of 0.83 for the 1999 data. It is quite likely that this significant increase in the quantity and range of data used would yield a more accurate determination of the true parameters.

It is important to note that there is not a complete consensus within the cosmology community that the expansion of the universe is accelerating. [Nielsen et al. \(2016\)](#) analyzed the robust type Ia SNe data from the SDSS-II/SNLS3 Joint Light-curve Analysis catalogue, and found that the data supports a *constant* rate of expansion. [Vishwakarma & Narlikar \(2010\)](#) critique the validity of statistical analysis performed in many of the evaluations of SNe data used to confirm the acceleration of the universe. They claim that many of these analyses rely too heavily on the assumption that their model is correct instead of using the data to directly assess the model. It is even possible that the assumption that the universe is isotropic on the large scale, which is foundational to our current cosmological model, is flawed. [Colin et al. \(2019\)](#) and [Bernal et al. \(2017\)](#) found that the previously discussed deceleration parameter - which defines the rate of acceleration of expansion - has a significant dipole component aligned with that of the CMB. This would mean that our universe is anisotropic. They suggest that the apparent acceleration in the SNe observed may be due to our being situated in a local bulk flow containing most of the SNe measured. However, in contrast to this, there has been extensive observational evidence for the accelerating universe apart from SNe observations. This evidence include measurements of the observational Hubble parameter, baryon acoustic oscillations and the CMB ([Haridasu, Balakrishna S. et al. 2017](#)). Evidently, more analysis and evaluation must be performed, not just on the SNe data, but also the models themselves.

5. CONCLUSIONS

The objective of this investigation is to determine the relative composition of the universe and thereby explore the rate of its expansion. We follow a similar procedure to the Nobel-Prize winning [Perlmutter et al. \(1999\)](#), using type Ia SNe as standard candles.

	Fit to 1999 Data	Fit to 2011 Data
Unconstrained Model	$\Omega_{M,0} = 0.30$ $\Omega_{\Lambda,0} = 0.91$	$\Omega_{M,0} = 0.73,$ $\Omega_{\Lambda,0} = 0.16$
Constrained Model	$\Omega_{M,0} = 0.55$ $\Omega_{\Lambda,0} = 0.45$	$\Omega_{M,0} = 0.58$ $\Omega_{\Lambda,0} = 0.42$

Table 1: Normalized energy densities of matter and dark energy found by fitting equation (2) to SNe data from both the 1999 and 2011 data-sets.

We analyze data from both their original data-set (published in 1999) as well as an updated 2011 data-set. We first fit a simplified model for $m_B(z)$ to the low-redshift ($z \leq 0.1$) data. We find the effective absolute magnitude in the B-band for type Ia SNe to be $\mathcal{M}_B = -3.19 \pm 0.07$. This was calculated as the average of the values from the fits to the 1999 and 2011 data, weighted by the coefficients of determination of the respective fits. Next, we develop a more complex general relativistic model for $m_B(z; \Omega_{M,0}, \Omega_{\Lambda,0})$, derived under the assumption of a flat universe. We fit the data to versions of this model both with and without the constraint

that $\Omega_{M,0} + \Omega_{\Lambda,0} = 1$. The results from the models fit to both the 1999 and 2011 data-sets are summarized in table 1.

The constrained fit to the 1999 data and both fits to the 2011 data suggest a mass-dominated universe. This is contradictory to the current generally accepted values of $\Omega_{M,0} \sim 0.3$ and $\Omega_{\Lambda,0} \sim 0.7$ (Suzuki et al. 2012). Results derived from the 2011 data are more reliable than those from the 1999 data, as the 2011 data-set contains many more SNe over significantly greater range of redshift values. When fit to this data, the unconstrained model suggests a highly mass-dominated *decelerating* universe, countering the general agreement within cosmology that the expansion of the universe is accelerating. As reviewed in the discussion section, there is not a unanimous consensus that the model of an accelerating universe driven by dark energy is correct. Further work must be done to probe this, which should include but must not be limited to type Ia SNe. As this important research continues, it is imperative that we perform rigorous statistical analysis and assess the validity of the assumptions upon which we are basing our models.

APPENDIX

A. DERIVATION OF MODEL

A.1. General Relativity Model

The Friedmann equation describes the expansion of space-time in a general relativistic model of a homogeneous and isotropic universe by

$$\left(\frac{\dot{a}}{a}\right)^2 = \frac{8\pi G\varepsilon(t)}{3c^2} - \frac{\kappa c^2}{R_0^2 a^2(t)}. \quad (\text{A1})$$

In this equation, G is the gravitational constant, c is the speed of light, R_0 is the radius of curvature of the universe, and κ is a dimensionless constant equal to +1, 0, or -1 for the cases of a closed, flat or open universe. The scale factor of the universe a defines how distances in space-time change over time through $r(t) = a(t)r_0$. In this equation, and in all contexts hereafter, the subscript 0 denotes evaluation at the current epoch ($t = t_0$). This scale factor relates to the Hubble parameter $H(t)$, which describes the rate of expansion of the universe, by

$$H(t) \equiv \frac{\dot{a}}{a}. \quad (\text{A2})$$

Finally, ε is the energy density of the universe defined by

$$\varepsilon(t) \equiv \varepsilon_M(t) + \varepsilon_R(t) + \varepsilon_\Lambda(t) \quad (\text{A3})$$

$$= \frac{\varepsilon_{M,0}}{a^3} + \frac{\varepsilon_{R,0}}{a^4} + \varepsilon_{\Lambda,0}, \quad (\text{A4})$$

where $\varepsilon_M(t)$, $\varepsilon_R(t)$ and $\varepsilon_\Lambda(t)$ are the energy densities of matter, radiation and dark energy, respectively. Using equation (A2) and applying the case of a flat universe, where $\kappa = 0$ and $R_0 = \infty$, equation (A1) becomes

$$H^2(t) = \frac{8\pi G\varepsilon_c(t)}{3c^2}, \quad (\text{A5})$$

where $\varepsilon_c(t)$ is the critical energy density for a flat universe. Evaluating equation (A5) at the current epoch yields

$$H_0^2 = \frac{8\pi G \varepsilon_{c,0}(t)}{3c^2}. \quad (\text{A6})$$

Then, dividing (A5) by (A6),

$$\frac{H^2(t)}{H_0^2} = \frac{\varepsilon_c(t)}{\varepsilon_{c,0}}. \quad (\text{A7})$$

The normalized energy densities of each component of the universe are given by

$$\Omega_{i,0} \equiv \frac{\varepsilon_{i,0}}{\varepsilon_{c,0}}, \quad (\text{A8})$$

where $i = M, R, \Lambda$ represent matter, radiation and dark energy, respectively. Using this definition, equation (A4) can be rewritten as

$$\varepsilon(t) = \varepsilon_{c,0}(\Omega_{R,0}(1+z)^4 + \Omega_{M,0}(1+z)^3 + \Omega_{\Lambda,0}), \quad (\text{A9})$$

where we have introduced the cosmological redshift z related to a by

$$a = \frac{1}{1+z}. \quad (\text{A10})$$

Substituting (A9) into (A7) and taking $\varepsilon(t) = \varepsilon_c(t)$ as this model applies to a flat universe,

$$H(t) = H_0 \sqrt{\Omega_{R,0}(1+z)^4 + \Omega_{M,0}(1+z)^3 + \Omega_{\Lambda,0}}. \quad (\text{A11})$$

At the current epoch, $\Omega_R \ll \Omega_M, \Omega_\Lambda$, so this can be approximated to

$$H(t) = H_0 \sqrt{\Omega_{M,0}(1+z)^3 + \Omega_{\Lambda,0}}. \quad (\text{A12})$$

A.2. Luminosity and Comoving Distance

The comoving distance r between two observers is the distance measure that does not change over time as it factors out the expansion of the universe. This comoving distance is given by

$$r \equiv \int_{t_e}^{t_0} \frac{cdt}{a(t)}. \quad (\text{A13})$$

Next, differentiating equation (A10) with respect to z gives

$$da = -\frac{dz}{(1+z)^2}. \quad (\text{A14})$$

Additionally, equation (A2) can be rewritten as

$$H(t) = (1+z) \frac{da}{dt}. \quad (\text{A15})$$

Then, substituting (A14) into this yields

$$dt = -\frac{dz}{H(z)(1+z)}. \quad (\text{A16})$$

This result can then be used to perform a substitution on equation (A13), noting that $z(t_e) = 0$ and $z(t_0) = z$, transforming it to

$$r = \frac{c}{H_0} \int_0^z \frac{dz'}{\sqrt{\Omega_{M,0}(1+z')^3 + \Omega_{\Lambda,0}}}. \quad (\text{A17})$$

If a source is emitting radiation at a comoving distance r , the observed energy flux will be

$$f = \frac{L_0}{4\pi r^2}, \quad (\text{A18})$$

where L_0 is the observed luminosity, related to the intrinsic luminosity of the source L_e by

$$L_0 = \frac{L_e}{(1+z)^2}. \quad (\text{A19})$$

The $1/(1+z)^2$ term accounts for the decrease in the photon energy caused by redshifting and the increase in the time interval between emission and observation. Equation (A18) can then be rewritten in terms of L_e as

$$f = \frac{L_e}{4\pi r^2(1+z)^2} \quad (\text{A20})$$

$$= \frac{L_e}{4\pi d_L^2}, \quad (\text{A21})$$

where we have defined the luminosity distance $d_L \equiv r(1+z)$. Finally, substituting equation (A17) for r into this definition of d_L yields

$$d_L = \frac{c(1+z)}{H_0} \int_0^z \frac{dz'}{\sqrt{\Omega_{M,0}(1+z')^3 + \Omega_{\Lambda,0}}}. \quad (\text{A22})$$

A.3. The Magnitude Scale

The standard magnitude scale gives the apparent magnitude of an astronomical object at a luminosity distance d_L to be

$$m = M + 2.5 \log \left(\frac{d_L}{10^{-5} \text{ Mpc}} \right)^2, \quad (\text{A23})$$

where M is the object's absolute magnitude, the apparent magnitude it would have were it located at a distance of 10 pc. Note that the use of Mpc in the denominator of the logarithmic term is to maintain consistent units with the Hubble Constant. This can be rewritten in terms of the "Hubble-Constant-free" luminosity distance $\mathcal{D}_L \equiv d_L H_0$:

$$m(z) = M + 5 \log_{10} \mathcal{D}_L - 5 \log_{10} H_0 + 25 \quad (\text{A24})$$

$$= \mathcal{M} + 5 \log_{10} \mathcal{D}_L, \quad (\text{A25})$$

where \mathcal{M} is the "zero point" modified absolute magnitude defined by $\mathcal{M} \equiv M - 5 \log_{10} H_0 + 25$. Writing this once again in terms of luminosity distance using equation (A22) yields

$$m(z) = \mathcal{M} + 5 \log_{10} \left[c(1+z) \int_0^z \frac{dz'}{\sqrt{\Omega_{M,0}(1+z')^3 + \Omega_{\Lambda,0}}} \right]. \quad (\text{A26})$$

In this investigation, absolute and apparent magnitudes in the blue band will be used, so equation (A26) will be henceforth written as

$$m_B(z) = \mathcal{M}_B + 5 \log_{10} \left[c(1+z) \int_0^z \frac{dz'}{\sqrt{\Omega_{M,0}(1+z')^3 + \Omega_{\Lambda,0}}} \right]. \quad (\text{A27})$$

This is the theoretical model that is fit to observational data in this paper.

REFERENCES

- Bernal, C., Cárdenas, V. H., & Motta, V. 2017, *Physics Letters B*, 765, 163, doi: [10.1016/j.physletb.2016.12.008](https://doi.org/10.1016/j.physletb.2016.12.008)
- Colin, J., Mohayaee, R., Rameez, M., & Sarkar, S. 2019, *Astronomy and Astrophysics*, 631, doi: [10.1051/0004-6361/201936373](https://doi.org/10.1051/0004-6361/201936373)
- Colin Cameron, A., & Windmeijer, F. A. 1997, *Journal of Econometrics*, 77, 329, doi: [https://doi.org/10.1016/S0304-4076\(96\)01818-0](https://doi.org/10.1016/S0304-4076(96)01818-0)
- Cottier, C. 2021, What shape is the universe? <https://astronomy.com/news/2021/02/what-shape-is-the-universe#:~:text=The%20theory%20of%20general%20relativity,the%20cosmos%20depends%20on%20it>.
- Haridasu, Balakrishna S., Luković, Vladimir V., D’Agostino, Rocco, & Vittorio, Nicola. 2017, *A&A*, 600, L1, doi: [10.1051/0004-6361/201730469](https://doi.org/10.1051/0004-6361/201730469)
- Nielsen, J. T., Guffanti, A., & Sarkar, S. 2016, *Scientific Reports*, 6, doi: [10.1038/srep35596](https://doi.org/10.1038/srep35596)
- Perlmutter, S. 2003, *Physics Today*, 56, 53–60, doi: [10.1063/1.1580050](https://doi.org/10.1063/1.1580050)
- Perlmutter, S., Aldering, G., Goldhaber, G., et al. 1999, *ApJ*, 517, 565, doi: [10.1086/307221](https://doi.org/10.1086/307221)
- Riess, A. G., Filippenko, A. V., Challis, P., et al. 1998, *The Astronomical Journal*, 116, 1009–1038, doi: [10.1086/300499](https://doi.org/10.1086/300499)
- Suzuki, N., Rubin, D., Lidman, C., et al. 2012, *The Astrophysical Journal*, 746, 85, doi: [10.1088/0004-637x/746/1/85](https://doi.org/10.1088/0004-637x/746/1/85)
- Tillman, N. T., & Harvey, A. 2022, What is cosmology? definition and history, *Space*. <https://www.space.com/16042-cosmology.html>
- Vishwakarma, R. G., & Narlikar, J. V. 2010, *Research in Astronomy and Astrophysics*, 10, 1195, doi: [10.1088/1674-4527/10/12/001](https://doi.org/10.1088/1674-4527/10/12/001)